Adaptation of the Mode Group Diversity Multiplexing Technique for Radio Signal Transmission Over Multimode Fiber

M. Awad, I. Dayoub, W. Hamouda, and J.-M. Rouvaen

***Abstract*—The large bandwidth of multimode fiber (MMF) makes it a very attractive medium for multiservice transmission in building networks at low cost. The mode group diversity multiplexing (MGDM) technique in graded-index multimode fiber (GI-MMF) has been shown to be less expensive with simpler transmitters and receivers, keeping the same information capacity. However, the classic transmission in MGDM complicates the integration of radio-over-fiber (RoF) services. In this paper, we propose a wired and a RoF model dedicated to broadband indoor applications. This model is based on a modified MGDM where we employ a variation of the transmission power technique and a selection algorithm for the optimal transmitter. To evaluate our system, the bit error rate and symbol error rate have been computed.**

***Index Terms*—MMF; Optical MGDM; Multiservice interference (MSI); Mixed services.**

I. INTRODUCTION

In-house, there is presently a wide variety of networks, each optimized for transporting a particular set of services [voice telephony, radio over fiber (RoF), etc.]. The lack of a common network infrastructure hampers the introduction of new services, and the creation of mutual relations among them. In short-reach optical networks, especially in local area networks (LANs), multimode fiber (MMF) links have been selected as the basic infrastructure [1]. Due to its large bandwidth, MMF seems to be the only medium able to offer broadband multiservices in the office and in in-door networks. A MMF network can constitute the backbone of the network, which feeds the fixed-wired services (such as data services gigabit Ethernet), as well as wireless services (IEEE 802.x, for example) in a single building using a multiplexing technique. To simultaneously transport various types of services [having various bandwidths, specific signal formats, diverse requirements in quality of services (QoS)], such a technique must meet a high efficiency/cost ratio.

Manuscript received February 25, 2010; revised September 20, 2010; accepted September 28, 2010; published December 7, 2010 (Doc. ID 124697).

M. Awad, I. Dayoub (e-mail: idayoub@univ-valenciennes.fr), and J.-M. Rouvaen are with the Université Lille Nord de France (UVHC-IEMN-DOAE, UMR CNRS 8520), Le Mont Houy, BP311, 59313 Valenciennes Cedex, France.

W. Hamouda is with Concordia University, Montreal, Quebec, Canada.

Digital Object Identifier 10.1364/JOCN.3.000001

There exist several conventional techniques, such as optical time-division multiplexing (OTDM), for the implementation of multiservice networks over MMF. However, OTDM is limited by the difficulty of generating short impulses. Therefore, the use of the OTDM technique in in-door networks is limited by the modal dispersion of the fiber, which widens the optical impulses. In addition, recovery of the synchronization signal at the receiver is difficult due to both modal dispersion and phase shift.

On the other hand, wavelength-division multiplexing (WDM) is known to improve the network capacity, and it enables the integration of different services in a single-MMF network, allowing the optimal use of the optical bandwidth [2]. This technique is limited by the capacity to generate an adequate optical carrier and correct data transmission at acceptable distances. Indeed, WDM requires wavelength-specific sources in addition to wavelength-selective network functions, which are still quite costly [3].

Optical code-division multiple access (O-CDMA) is another candidate for multiservice systems with high capacity. The application of direct sequence CDMA (DS-CDMA) with the MMF has been demonstrated in [4]. However, spread spectrum with high flow rates (10 Gb/s) requires the use of lasers at high frequencies, which renders the system more expensive. Indeed, time-spreading CDMA for RoF systems might need code or carrier synchronization. In [5], a bandpass sampling technique with an aliasing canceler has been introduced to improve the carrier-to-interference ratio (CIR).

Subcarrier multiplexing (SCM) allows the transmission of various services with simple detection and efficiently exploits the bandwidth of the fiber. This technique is based on the generation of various electric subcarriers associated with various signals. These carriers are then combined and used to modulate an optical carrier [6]. However, the use of a similar communication technique, as in the case of the SCM, is more sensitive to the effects of noise and distortion due to the nonlinearities of the MMF. Moreover, these conventional techniques do not take into consideration the intermodal dispersion, where system performance is still limited to low bit rates and short distances.

Another technique known as mode group diversity multiplexing (MGDM) has been introduced recently to replace the

1943-0620/11/010001-9/$15.00

more expensive WDM in LAN networks. The idea behind this technique arises from a recently developed wireless transmission scheme known as the basic local alignment search tool (BLAST) [7]. The MGDM is a multiplexing technique, based on the spatial launching and detection of subgroups of modes to create a number of independent communication channels in a single MMF. This technique exploits the unused capacity of MMF for improving the bandwidth $\times$fiber length product. In MGDM, the excitation of subgroups of modes decreases the intermodal dispersion, resulting in up to a fourfold bandwidth increase by exciting less than 50% of the fiber modes [8]. In that, every transmitter launches a defined mode group (MG), which is detected by a spatial receiver placed at the end facet of the fiber. However, the MG propagation in each channel is not ideal. This is due to subgroup mode mixing and nonorthogonality of transmitters and receivers, which causes crosstalk between propagation channels producing multiservice interference (MSI). To separate the services, electrical signal processing is required after the optoelectronic conversion.

MGDM with multiple input and multiple output is similar to multiple-input–multiple-output (MIMO) systems in radio communications. The digital signal processing (DSP) used in radio networks to mitigate the effects of multiple channels can be used to mitigate the MSI in optical networks employing MGDM. Yet, efficient algorithms and hardware implementations are needed to facilitate the separation of services after the optoelectronic conversion. For MGDM, the simplest receiver architecture is based on matrix inversion, a zero-forcing (Z-F) equalizer in line with the requirement of service transparency [9].

Koonen *et al.* in [10] have pointed out the challenges of the MGDM application for radio services. The electrical part of the receiver and processing electrical signal (i.e., Z-F) complicate the integration of radio services. In this paper, we demonstrate the possibility of adapting this technique for radio services. For this purpose, we present a modified MGDM model for radio signal transmission in the presence of baseband signals. This model incorporates the idea of the optimal antenna selection in MIMO radio systems [11].

The paper is organized as follows. In Section I, the classical MGDM technique description is given. In Section II, we review the algorithm of orthogonal channels in the modified MGDM system. In Section III, we present a modified MGDM system with simulation results. Finally, the discussion in Section IV provides perspective on the key points.

II. Classical MGDM Technique Description

Several scenarios are studied to realize an optical MIMO system at low cost. Coherent optical MIMO (CO-MIMO), presented in [12], is based on the coherent optical system and its potential to exploit the inherent information capacity of the MMF. The use of directional couplers allows different mode groups to be launched and received in order to reduce the correlation among subchannels. But even with these simple coupling techniques at the input facet of the fiber, their use launches a large number of propagation modes. In this case, the intermodal dispersion remains significant, and CO-MIMO does not improve the transmission quality in an obvious manner.

The MGDM technique with a spatial coupler and receiver can allow for the launch of limited subgroup modes (SGMs) associated with each transmitter. This technique reduces the intermodel dispersion by keeping the high capacity of the system and maintaining orthogonality between several channels. Each transmitter is characterized by two parameters, offset and spot size: the offset (F) is the transmitter position according to the central axis of the propagation in the fiber, and the spot size (w) is the size of the incident light beam on the input facet of the fiber. Once these two parameters are determined, it is possible to launch the light source with a given angle (θ: angular offset) in order to obtain $\eta = 100\%$ efficiency [13]. In our work, we took into account the angular offset as mentioned to minimize the power loss. Also the realization of transmitters is possible through single-mode fibers (SMFs) associated with each user, with its radius determining the spot size [14]. For example, for a MGDM (3×3) system, almost three separate channels are created in a GI-MMF (62.5/125) by the injection of the light in three different offsets: $F=0, 13, 26$ μm. Figure 1 shows the excitation profile of SGMs and the power distribution according to these three offsets.

The central transmitter ($F=0$) launches only lower-order modes (LMs) (in the ideal case, the lowest mode will carry more energy). For the launching of the light at $F=13$ and 26 μm (extremity channels), higher-order modes (HMs) are excited, which are mainly traveling in the outer region of the MMF core. However, the propagation of SGMs associated with each channel along the fiber is not totally independent. A "modes mixing" between the various SGMs causes channel overlapping and degrades the orthogonality of the system. At the reception, every SGM has a specific area of optical energy distribution at the output facet of the fiber. Figure 2 shows the intensity distribution of the light flux of the three channels in the plane perpendicular to the axis of the fiber propagation with $L=100$ m.

For the fundamental channel ($F=0$ μm), the light energy is concentrated in a zone at the middle of the fiber core. But the light energy at the extremity channels is distributed in

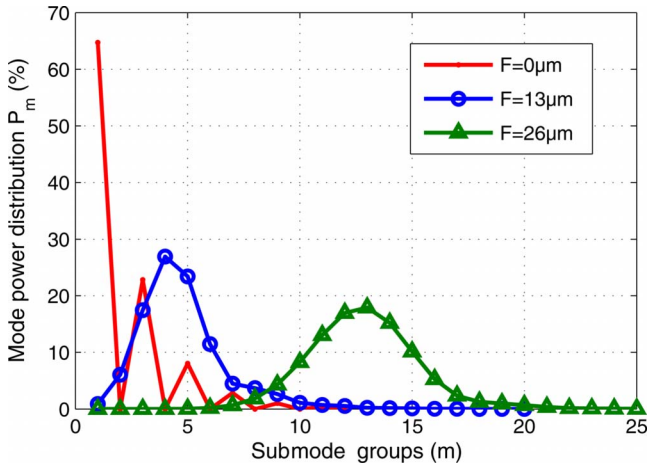

Fig. 1. (Color online) Excitation profile at the input facet of GI-MMF (62.5/125) for three offsets with $w=4$ μm.

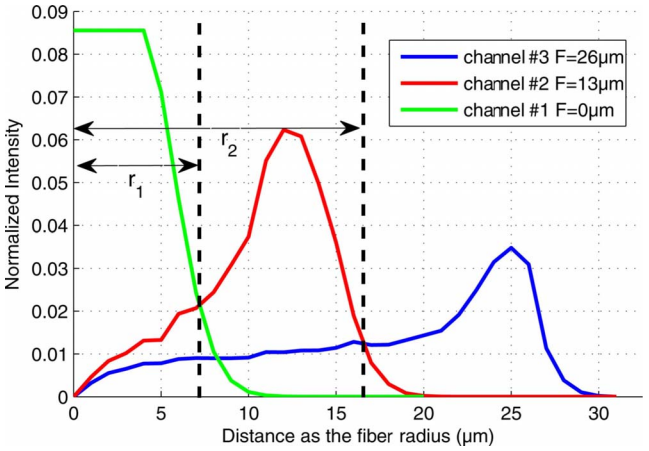

Fig. 2. (Color online) Light intensity distribution for three excitation positions ($F=0,13,26$ μm).

the outside region of the core. The reception part can be achieved by using a lens placed on the output facet of the fiber, for the projection of the optical light onto an optoelectronic integrated circuit (OIC), which employs photodetectors and preamplifiers (PDIC) [13].

For a MIMO radio system, the relationship between antennas at reception and emission is presented in matrix form. Similarly for an O-MIMO system, the relationship between receivers and transmitters is presented analytically by a matrix. Elements of this matrix present the subchannels in the fiber. The relationship between the N received electrical signals (y_i) and the N emitted electrical signals (s_i) is written in the form

$$\begin{pmatrix} y_1 \\ y_2 \\ \vdots \\ y_N \end{pmatrix} = \begin{pmatrix} h_{11} & h_{12} & \cdots & h_{1N} \\ h_{21} & \ddots & \cdots & h_{2N} \\ \vdots & \cdots & \ddots & \vdots \\ h_{N1} & h_{N2} & \cdots & h_{NN} \end{pmatrix} \cdot \begin{pmatrix} s_1 \\ s_2 \\ \vdots \\ s_N \end{pmatrix} + \begin{pmatrix} n_1 \\ n_2 \\ \vdots \\ n_N \end{pmatrix} \tag{1}$$

or in matrix notation as

$$\mathbf{y} = \mathbf{H} \cdot \mathbf{s} + \mathbf{n}, \tag{2}$$

where $\mathbf{y}$, $\mathbf{s}$, $\mathbf{n}$ are, respectively, the received signal vector, the emitted signal vector, and the additive noise from the receivers. The matrix elements h_{ij} describe the signal transfer from the transmitter i to the detector j. Each element has an amplitude [representing the path mitigation (i,j)] and a phase [corresponding to the delay of the specific path (i,j)]. In the case of MGDM with negligible modal dispersion, the coefficients h_{ij} take real values, expressing the proportion of power transmitted by the ith source and received by the jth detector [13].

In [15], we have presented an analytical model of the MGDM ($N\times N$) system. This model is based on the resolution of propagation equations in the multimode fiber. A transmitter modelization by a Gaussian field is followed by a determination of the SGM launched by every transmitter according to the pair (w,F) (determination of the modal amplitude coefficients by the overlap integral between the electric field of the SMF and that of the MMF). At reception, the output facet of the fiber is divided into N sections, followed by the determination of the light flux intensity in each area. The distribution of N light fluxes over N sections allowed us to determine the coefficients of the matrix $\mathbf{H}$. This model is followed by a complete study of spatial emission and reception conditions in order to increase the orthogonality between channels and to maximize the system capacity. Moreover, by using this model, we evaluated the MMF MGDM system performance for various numbers of users. The results indicate a BER $<10^{-10}$ for a 5×5 MGDM system for a 5 Gb/s bit rate over several hundred meters of MMF. The coupling effects on MMF are divided into intermode and intramode mixing. Intramode mixing depends on the light source and occurs between modes of the same SGM. Intramode mixing is the major effect in MMF transmission apart from external factors acting on the fiber. The modeling of the intramode mixing method is presented in [14], where the power is distributed evenly among the SGMs. The intermode mixing occurs between different SGMs (produced by external effects on the fiber: curvature, microcurvature, etc.). Note that intermode mixing increases MSI. In our previous work [15], we developed a theoretical model including the modeling of curvature effects of installed fiber, due to a mechanical deformation, producing intermode mixing. In addition, we have also considered the radius of curvature (R_c) equal to the minimum radius ($R_{\min}$) provided by the installers. We found that the MGDM system maintains good performance if $R_c > R_{\min}$, and otherwise the system performance degrades [e.g., the MGDM (3×3) is 300 m for $D=10$ Gb/s, and the BER varies from 10^{-12} to 10^{-7} for a strong curvature].

The work that we present in this paper is based on the use of this demonstrated model with optimal emission and reception conditions as illustrated below. Also in this work we take into account the intramode mixing effects.

III. Modified MGDM Algorithms

The classical MGDM system is based on equal optical powers for all channels in the system. In addition, the model architecture of the classical MGDM system is adapted for baseband service transmission. The modification of this architecture at the transmitter or the receiver allows us to add radio services to the system. The aim of such an architecture modification is to maintain an orthogonality between radio services (launched on a single transmitter) and other baseband services. The orthogonality here means an aggregate of baseband signals without influence from the radio signal. Thus, the received radio signal is transmitted at the end user without modification. In addition, the orthogonality is maintained among all services.

In a previous work (i.e., European Project ROSETTE), we demonstrated that all radio standards of the second and third generations (i.e., GSM, UMTS, Wi-Fi, etc.) can be transmitted over one fiber with high QoS where the fiber behaves as a simple transport medium (without any radio signal processing) [1]. Indeed, all radio signals are emitted over the fiber using just one MIMO channel (offset=0).

In [16] we presented a model of modified MGDM by an orthogonality at the receiver. The reception of the radio signal (carrier frequency: $f_p=2.5$ GHz) launched at the central transmitter is followed by an electrical bandpass filter after

the optoelectronic conversion. On the other hand, the reception of baseband signals is followed by low-pass filtering techniques controlled by their bit rates ($D=1$ Gb/s) to separate them from the radio signal. However, the use of this system for a radio signal and for a baseband signal, both having the same frequency band, is complicated. For example, the transmission of a GSM signal with $f_p=1$ GHz and a baseband signal with $D=1$ Gb/s on the same fiber by the use of the MGDM technique complicates their separation by filtering systems at the reception.

Here we propose a technique, based on orthogonality, that can be adapted at the emission part. This approach is based on techniques similar to those used in MIMO radio systems for optimal antenna selection [17]. A selection criterion of the suboptimal antenna is used in the case of the linear and coherent receivers: a signal-to-noise ratio (SNR) postprocessing of the multiplexed stream, which involves choosing the antenna that results in the minimum SNR as being the optimal antenna. Therefore, using the optimal antenna (lowest power) for data emission leads to good performance in terms of probability of error. The aim of optimal antenna selection in radio MIMO systems is mainly to improve transmission quality. In our study, we will take part in this study (selection of optimal transmitter) in the optical case, to associate the optimal transmitter of radio signals. We will adapt a selection algorithm to create orthogonality at the receiver side of the MGDM system. Note that the selection algorithm in radio systems is only suitable for a sufficiently slow time-varying channel. In the optical MIMO system, especially when using MGDM, the coefficient of the **H** matrix varies slowly in time compared with the symbol period. The effects of temperature on MGDM have been studied in [18]. It is noted that the temperature acts slowly on both SMGs and the redistribution of the modal power. The strategies for adapting the **H**-matrix coefficients can be dynamically designed. These variations can be monitored by adding some redundancy to the transmitted signals using online coding. These codes allow the detection of transmission errors at the receiver. If too many errors occur, the receiver may request through a feedback channel to the transmitter to send another training sequence for a new system initialization.

The analytical model describing the relation between transmitted and received signals presented in Eq. (1) for the MGDM system can be modified and written as follows:

$$\begin{pmatrix} y_1 \\ y_2 \\ \vdots \\ y_N \end{pmatrix} = \begin{pmatrix} h_{11} & h_{12} & \cdots & h_{1N} \\ h_{21} & \ddots & \cdots & h_{2N} \\ \vdots & \cdots & \ddots & \vdots \\ h_{N1} & h_{N2} & \cdots & h_{NN} \end{pmatrix} \cdot \begin{pmatrix} s_1 \\ s_2 \\ \vdots \\ s_N \end{pmatrix} + \begin{pmatrix} h_{1r} \\ h_{2r} \\ \vdots \\ h_{Nr} \end{pmatrix} \cdot s_r + \begin{pmatrix} n_1 \\ n_2 \\ \vdots \\ n_N \end{pmatrix} \tag{3}$$

or in compact form as

$$\mathbf{y} = \mathbf{H}_1 \cdot \mathbf{s}' + \mathbf{H}_2 \cdot \mathbf{s}_r + \mathbf{n}. \tag{4}$$

The transfer matrix **H** is decomposed into two parts: $\mathbf{H}_1$, which represents the channel matrix associated with baseband services $s' = \{s_2, s_3, s_{r-1}, s_{r+1}, \ldots, s_N\}$, and $\mathbf{H}_2$, the channel matrix associated with radio services (s_r). The idea is to create a maximum orthogonality between $\mathbf{H}_1$ and $\mathbf{H}_2$ at the transmitter side. To achieve this goal, we have introduced two criteria: the power criteria to protect baseband services and the choice of the optimal transmitter criteria to enable radio services transmission.

A. Power Criteria

Before the launching of various services in the fiber, it is possible to protect baseband services by the variation of optical powers. This power variation allows the overlapping of subchannel $\mathbf{H}_2$ over $\mathbf{H}_1$ to be decreased. Indeed, each receiver captures a mix of signals. For example, receiver x will capture the fundamental signal in demand (s_x), consisting of a mixture of baseband signals and that of the radio signal,

$$y_x = \underbrace{h_{x2}s_2 + \cdots + h_{xx}s_x}_{BB\ Signals\ (I_1)} + \underbrace{h_{xr}s_r + n_x}_{Radio\ Signal\ (I_2)+noise}. \tag{5}$$

To recover the data stream $\hat{s}_x$ at reception, it is necessary to reduce the overlap with the radio signal (I_2) before separating baseband signals (I_1) by electrical signal processing. For this purpose, we suppose that the radio signal forms an additive noise acting on the receiver x (i.e., the product $h_{xr}s_r$ presents a noise that affects the received signal y_x). For the radio signal to be considered as additive noise, it is necessary that $I_2 \ll I_1$. For that, we have considered two factors: the optical power of the radio signal and the coefficient h_{xr}.

The radio signal is launched at the transmitter side with an average optical power P_1, while each baseband signal is launched with an average power P_2 such that $P_2 > P_1$. For that purpose, let us define the power ratio α as follows:

$$\alpha = \frac{P_2}{P_1}, \tag{6}$$

with $\alpha > 1$.

The choice of average powers (P_1,P_2) at emission is related to the product (I_2,I_1) at reception and the additive noise (n_2) with the following relationship: $n_2 \ll I_2 \ll I_1$. Note that the noise element n_2 is the additive noise affecting the receiver R_2 resulting from the optoelectronic component.

In an optical reception system, the element with the highest noise is the photodiode. n is a thermal noise due to random movements of electrons in any conductor. Mathematically, this intrinsic thermal noise in a conductor of resistance R is modeled as a Gaussian random process with one-sided spectral density given by

$$N_{th} = \sqrt{\frac{4K \cdot T \cdot B}{R}}. \tag{7}$$

Note that the choice of the optimum transmitter associated with the radio signal can decrease the correlation factors h_{xr} as well as I_2, where the coefficient h_{xr} represents the influence of the radio signal on the receiver x.

B. Choice of the Optimal Transmitter Criteria

To protect the radio signal [launched with low power (P_1)] and to increase the orthogonality at reception with other signals, it is necessary to launch it on an optimal channel. We define the factor of the total optical crosstalk (σ_i) at the reception area R_i as

$$\sigma_i = 10 \cdot \log_{10}\left(\left(\sum_{i\neq j} h_{i,j}\right) \Big/ (h_{i,i})\right), \tag{8}$$

where the coefficient σ_i measures the orthogonality between receivers and depends on the values of the matrix coefficients **H**. The values of coefficients h_{ij} are given by [15]

$$h_{ij} = \frac{I_j(R_i,L)}{I_j(R,L)}, \tag{9}$$

where I_j is the light flux intensity emitted by the jth transmitter, R_i is the area of the jth receiver, R is the total area of the core fiber, and L is the fiber length. The light flux intensity is given by

$$I(R,L) = \frac{1}{2}\sum_{\mu,\nu} |a_{\mu,\nu}(L)|^2 \int_R \Psi_{\mu,\nu}^2 \mathrm{d}s + \sum_{\mu\neq\mu'\,\nu\neq\nu'} \left[a_{\mu,\nu}(L)\cdot a_{\mu',\nu'}(L) \times \int_R \Psi_{\mu,\nu}\Psi_{\mu',\nu'}\mathrm{d}s \right] \cos((\beta_{\mu,\nu} - \beta_{\mu',\nu'})L), \tag{10}$$

where $a_{\mu,\nu}$ and $\Psi_{\mu,\nu}$ are respectively the modal amplitude and the modal function of the (μ,ν) mode. $\beta_{\mu,\nu}$ is the propagation constant. Note that the optical crosstalk (σ_i) depends on the area R_i $(\sigma_i = f(R_i))$.

We take the example of an MGDM (4×4) system for both types of GI-MMF (50/125 and 62.5/125). By determining σ_i of each receiver $R_i \in \{R_1,\ldots,R_4\}$, we can determine the optimal channel (Fig. 3), the one with the minimum value of σ_i.

Figure 3 shows that receivers R_1 and R_4 are less affected by other signals [$\sigma_1 < -3$ dB, $\sigma_4 < -5$ dB for the MMF (62.5/125)]. These two receivers are associated with the central ($F=0$ μm) and eccentric transmitters ($F=26$ μm), respectively. These two transmitters can represent the optimal choice for the radio signal transmission. However, the choice between these two transmitters depends on their orthogonality, such that the product $I_2 = h_{xr}s_r$ will be the lowest possible. By comparing the partial optical crosstalk of the fundamental channel $(\sigma_{1x} = 10\log_{10}(h_{x,1}/h_{x,x}))$ of each receiver with that of the extremity channel $(\sigma_{3x} = 10\log_{10}(h_{x,3}/h_{x,x}))$, we can determine the optimal transmitter of the system (Fig. 4).

Figure 4 shows that the influence of the fundamental transmitter on R_2 is lower than that of the eccentric transmitter [$F=26$ μm, for MMF (62,5/125)] ($\sigma_{12} = -7$ dB and $\sigma_{32} = -3$ dB). Moreover, the effect of the fundamental transmitter on the extremity receiver (R_3) is lower than the inverse effects of the eccentric transmitter on the receiver R_1 ($\sigma_{13} = -28$ dB and $\sigma_{31} = -9$ dB). The low influence of the signal associated with the fundamental transmitter on all receivers renders this as the optimal transmitter. Given this, the product I_2 decreases, which allows us to consider this product as an additive noise. Such noise is then added with the noise of optoelectronic components on the receivers associated with the baseband signals. In addition, we have shown in [15] that the fundamental channel delivers good performance even in the presence of external disturbances acting on the fiber. This is important to protect the radio signal launched with a low optical power.

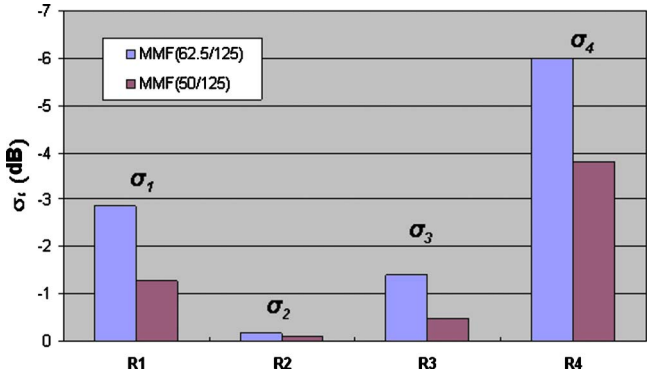

Fig. 3. (Color online) Crosstalk σ_i associated with each receiver (R_i) for a 4×4 system.

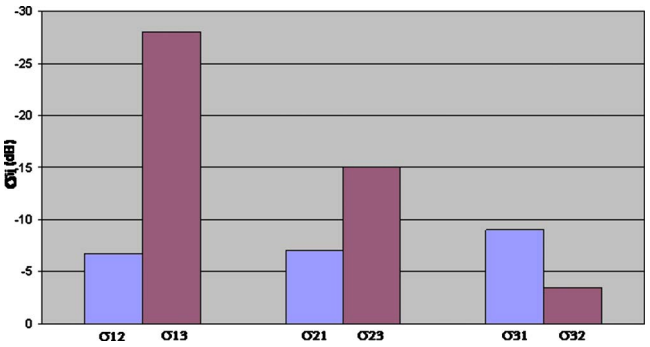

Fig. 4. (Color online) Partial optical crosstalk for the MGDM (3×3) system.

On the other hand, the radio signal (s_1) is received by the fundamental receiver (R_1) with a mixture of other service interference and an additive noise:

$$y_1 = \underbrace{h_{11}s_1}_{\lambda_1} + \underbrace{h_{12}s_2 + \cdots + h_{1N}s_N}_{\lambda_2} + n_1. \tag{11}$$

We should note that signal processing after the receiver R_1 to recover the radio signal complicates the system. Also it is necessary to recover the radio signal and send it to the end user without alteration. In order to protect the radio signal from overlapping with other users' signals, we propose to send a radio signal on an optical carrier (λ_1), and other signals on a different wavelength (λ_2). To maintain better quality of transmission of the radio signal, we use an optical filter at λ_1 to recover the radio signal at the receiver R_1.

Note that the classic emission of the MGDM system with an equal power and an optical frequency (P, λ) is modified by a dual power (P_1, P_2) and a dual optical carrier (λ_1, λ_2). Figure 5 shows the change in the distribution of the average

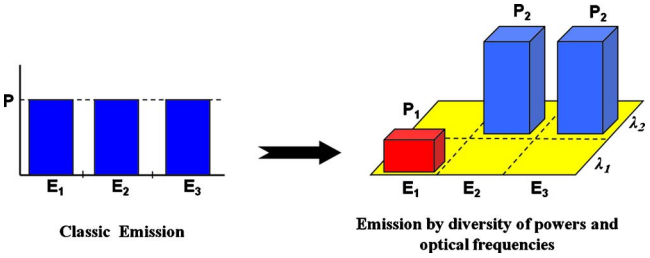

Fig. 5. (Color online) Emission with various average optical powers and wavelengths.

optical power by the users at the input facet of the fiber for a MGDM (3×3) system. The matrix coefficients **H** describe the spatial distribution of optical power or the ratio of the emitted power on a given surface. Their values do not change by the variation of power and the wavelength on various channels.

Note that, by comparing the WDM with the modified MGDM for an ($N\times N$) system, WDM requires N optical filters at the reception part, whereas our model needs only one filter dedicated to radio services.

IV. Modified MGDM System Application and Simulation

Here, we analyze the system performance of the modified MGDM communication link model in Section 3, including the radio signal and several baseband signals. For $N\times N$ MGDM systems, we simulated the average BER and SER for several system configurations with different numbers of users, power factor α, and SNR. The simulated model is shown in Fig. 6.

Our simulation chain is carried out using the VPI software. We assume N independent inputs: one radio signal and $N-1$ baseband signals. To demonstrate that we can obtain good-quality radio frequency transmission over MMF, with the MGDM technique, we used 16-QAM for the radio signal. In our simulations we consider a carrier frequency of 2.5 GHz, with a bit rate set to 32 Mb/s (IEEE 802.11 g standard). Optoelectronic transpositions have been realized by a $\lambda_1=1300$ nm laser providing an optical power P_1. The radio signal is emitted into the central transmitter ($F=0$ μm, channel #1). On the other side, each baseband signal is on–off keying (OOK) modulated by an independent pseudorandom binary data stream (2.5 Gb/s). Each laser, associated with a user, modulates the binary data at the same wavelength ($\lambda_2=1315$ nm) with the same power (P_2). By cosimulation using Matlab and VPI, we introduce the MGDM channel model presented in [15].

At the receiver, each photodiode captures a mixture of signals. The central receiver R_1 is followed by an optical filter to recover the radio signal that will be sent after the electro-optical conversion to the end user. Photodiodes for the receiver R_2 to R_N are followed by electrical signal processing to recover the baseband signals. For MGDM, the simplest receiver architecture is matrix inversion, a Z-F method in line with the requirement of service transparency. From Eq. (4) the relation between the signals is given by

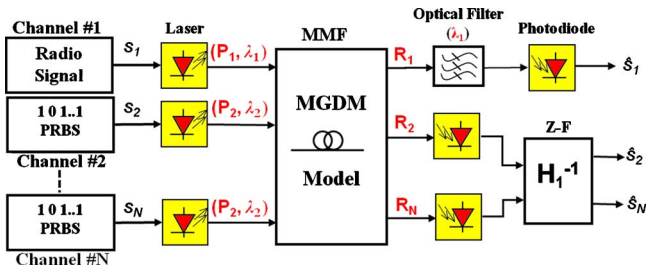

Fig. 6. (Color online) M-MGDM model.

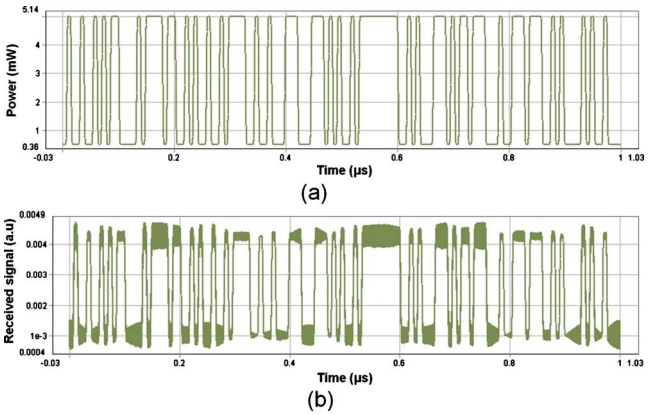

Fig. 7. (Color online) Waveform signal: (a) emitted signal (mW), (b) electrical received signal.

$$\widehat{\mathbf{s}'} = \mathbf{s}' + \mathbf{H}_2\mathbf{H}_1^{-1}\cdot\mathbf{s}_r + \mathbf{n}\mathbf{H}_1^{-1}. \tag{12}$$

Figure 7 shows a baseband signal emitted in a modified MGDM (2×2) system (MMF 50/125) and an equivalent signal at reception (receiver R_2). The received signal shows the overlap of the radio signal for $\alpha=2$.

For our simulation, we study the performance of the system by measuring the BER after equalization (Z-F) and by measuring the SER for the radio signal after filtering. For an M-MGDM (3×3) system [MMF (50/125), fiber length $L=800$ m], we estimated the BER of the baseband signal at reception according to the factor α and by varying the average emitted power (Fig. 8). With low power ($P_2=-19$ dBm), the BER is very high, even for high values of α. However, with $P_2=-14$ dBm, and for $\alpha=5$, BER$<10^{-9}$.

Note that the radio signal interference on channel #2 becomes low for $\alpha>5$. In addition, we have drawn the worst-case scenario when both the baseband and radio frequency signals are in the same bandwidth (e.g., 2.5 GHz), where radio frequency signal impacts are maximum on the baseband. When the frequency offset between the radio fre-

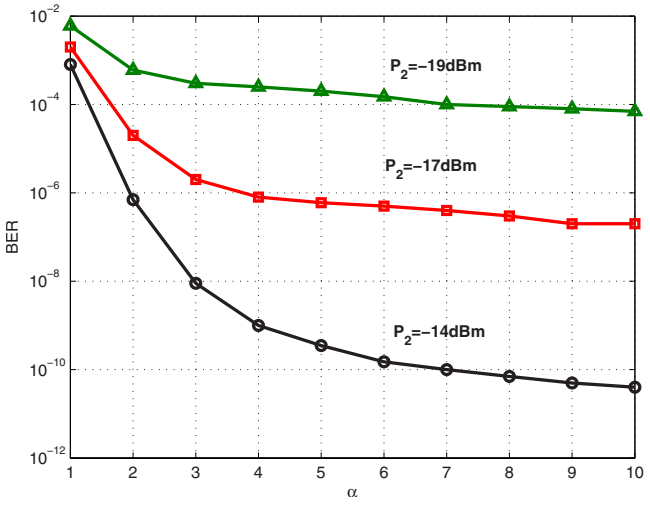

Fig. 8. (Color online) BER according to the factor α for several emitted powers P_2.

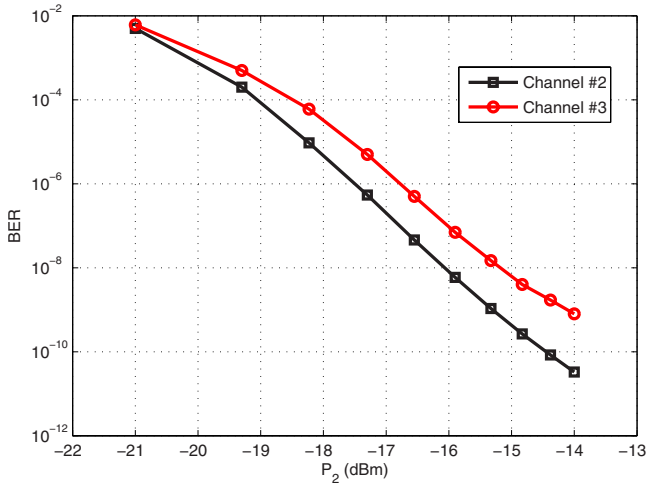

Fig. 9. (Color online) Comparison of BER for two extremity channels.

quency signal and the baseband is large (i.e., 1 GHz), then we can use smaller values of α.

In Fig. 9 we compare the BER calculated for the signal associated with the second ($F=10$ μm) and third transmitters ($F=19$ μm), respectively. Figure 9 shows a comparison of BER according to the average power at emission by taking an average power factor of $\alpha=5$.

The difference of the BER for both channels shows that the transmitter associated with channel #2 ($F=10$ μm) results in slightly better performance than the one for channel #3 ($F=19$ μm).

Until now, we have shown only the performance for baseband signals, which vary according to the average optical power associated with the radio signal transmitter. In what follows, we present the performance of the radio frequency signal in our model. After an optoelectronic conversion and demodulation of radio signals at reception, we calculate the SER. By calculating the SER according to the variation of the factor α with low powers at emission P_2, we obtain the results presented in Fig. 10 for MGDM (3×3).

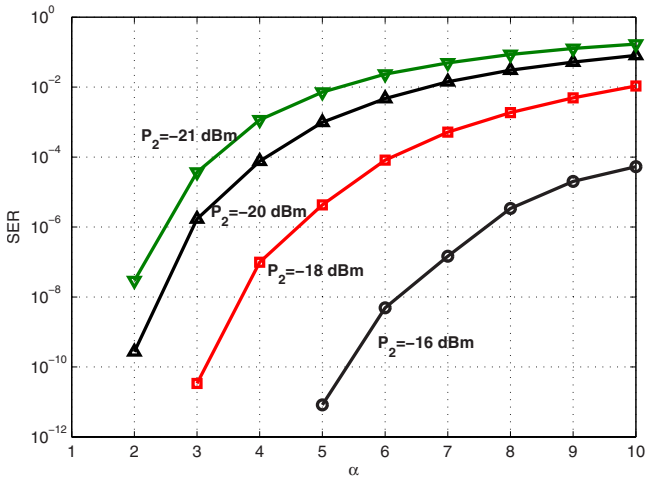

Fig. 10. (Color online) SER according to the factor α for several input powers P_2.

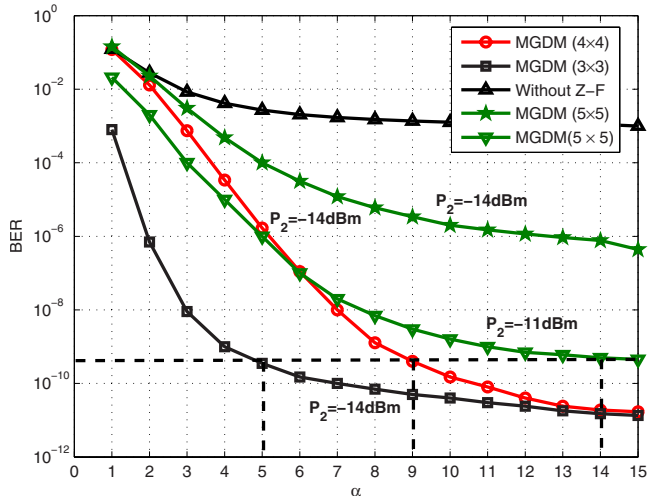

Fig. 11. (Color online) BER according to α for 3×3, 4×4, and 5×5 systems.

From Fig. 10, for a low power factor α, the best performance is obtained for the radio signal, even for low powers. Also, for low input power ($P_2=-21$ dBm), the performance degrades for high values of α (SER$\simeq10^{-2}$ for $\alpha=5$). But, for a power of $P_2=-16$ dBm, the best performance is obtained even for low values of α (SER$<10^{-10}$ and SER$=5\times10^{-5}$ for $\alpha=5$ and $\alpha=10$, respectively).

Note that the transmission of radio signals and baseband signals (3×3) is guaranteed by the use of our model: for $\alpha=5$, SER$<10^{-9}$ and SER$<10^{-10}$ for the baseband signal ($D=2.5$ Gb/s) and radio signal ($f_p=2.5$ GHz), respectively. It is clear that increasing the radio signal frequency degrades the radio signal quality (SER). Therefore, at higher radio signal frequency, we can use smaller values of α.

Moreover, the choice of the factor α varies with the number of users. We compared the performance of the baseband signal (channel #2) in a 3×3 system with that of 4×4 and 5×5 systems. Figure 11 depicts this comparison for average input powers of $P_2=-14$ and -11 dBm.

From Fig. 11, we can see that the product $I_2=h_{x,1}s_1$ varies according to the number of users and $h_{x,1}$ becomes higher since receivers are spatial detectors. In addition, the distance between receivers decreases with the number of users, and interference among signals increases, especially that of the radio signal. For a BER$\simeq10^{-10}$, the power factor varies with the number of users: $\alpha=5$ and 9 for 3×3 and 4×4, respectively, with $P_2=-14$ dBm. But, with this power ($P_2=-14$ dBm), the BER does not reach 10^{-7} for the 5×5 system. Also for an emission with an average power $P_2=-11$ dBm, we obtained a BER$\simeq10^{-10}$ for the 5×5 system with $\alpha=14$.

V. Summary and Discussion

The transmission of different services by a multimode fiber using the MGDM technique is effective in in-door networks. We studied the possibility of using this technique for transmission of radio services with baseband services (Ethernet, for example). One problem in this case is the detection of the radio signal by the equalizer. To solve this prob-

lem, we have presented a model based on the launching of services with a difference in optical power. In our system, the radio signal is emitted on the optimal channel to protect baseband services. We demonstrated by simulation, with the adaptation of the radio signal with baseband signals, that better performance for baseband signals are achieved: BER$<10^{-10}$ for $D=2,5$ Gb/s in M-MGDM (3×3) system over several hundred meters of MMF. We have also demonstrated the best performance for the radio signal, even with low optical powers.

REFERENCES

[1] I. Dayoub, A. Zaouche, J.-M. Rouvaen, C. Lethien, J.-P. Vilcot, and D. Decoster, "Radio-optic demonstrator for distributed antenna system indoor wireless applications using low-cost VCSELs," *Eur. Trans. Telecommun.*, vol. 18, no. 7, pp. 811–814, 2007.

[2] L. B. Aronson, B. E. Lemoff, L. A. Buckman, and D. W. Dolfi, "Low-cost multimode WDM for local area networks up to 10 Gb/s," *IEEE Photon. Technol. Lett.*, vol. 10, pp. 1489–1491, 1998.

[3] X. J. Gu, M. Waleed, and P. W. Smith, "Demonstration of all-fiber WDM for multimode fiber local area networks," *IEEE Photon. Technol. Lett.*, vol. 18, no. 1, pp. 244–246, 2006.

[4] A. Okassa-M'foubat, I. Dayoub, and J. M. Rouvean, "Impact of modal dispersion on the parallel interference cancellation in DS-CDMA optical networks," in *the 7th IASTED Int. Conf. on Communication Systems and Networks*, Spain, 2008, pp. 102–106.

[5] B. K. Kim, S. Park, Y. Yeon, and B. W. Kim, "Radio-over-fiber system using fiber-grating-based optical CDMA with modified PN codes," *IEEE Photon. Technol. Lett.*, vol. 15, no. 10, pp. 1485–1487, 2003.

[6] A. Stohr, K. Kitayama, and D. Jager, "Full-duplex fiber-optic RF subscarrier transmission using a dual-function modulator/photodetector," *IEEE Trans. Microwave Theory Tech.*, vol. 47, no. 7, pp. 1338–1341, 1999.

[7] G. D. Golden, C. J. Foschini, R. A. Valenzuela, and P. W. Wolniansky, "Detection algorithm and initial laboratory results using V-BLAST space-time communication architecture," *Electron. Lett*, vol. 35, no. 1, pp. 14–16, 1999.

[8] L. Raddatz, I. H. White, D. G. Cunningham, and M. C. Nowell, "An experimental and theoretical study of the offset launch technique for the enhancement of the bandwidth of multimode fibre links," *J. Lightwave Technol.*, vol. 16, no. 3, pp. 324–331, 1998.

[9] T. Koonen, H. van den Boom, I. T. Monroy, and G.-D. Khoe, "High capacity multi-service in-house networks using mode group diversity multiplexing," in *Optical Fiber Communication Conf.*, Los Angeles, 2004, pp. 22–27.

[10] A. M. J. Koonen, H. P. A. van den Boom, A. Ng'oma, M. Garcia Larrode, J. Zeng, and G.-D. Khoe, "POF application in home systems and local systems," in *Conf. on Polymer Optical Fibre*, Hong Kong, 2005, vol. 1, pp. 165–168.

[11] D. A. Gore and R. W. Heath Jr., "Transmit selection in spatial multiplexing systems," *IEEE Commun. Lett.*, vol. 6, no. 11, pp. 491–493, 2002.

[12] A. R. Shah, R. C. J. Hsu, A. Tarighat, A. H. Sayed, and B. Jalali, "Coherent optical MIMO (COMIMO)," *J. Lightwave Technol.*, vol. 23, no. 8, pp. 2410–2419, 2005.

[13] C. P. Tsekrekos, A. Martinez, F. M. Huijskens, A. M. J. Koonen, "Mode group diversity multiplexing transceiver design for graded-index multimode fibres," in *31st European Conf. on Optical Communication*, 2005, vol. 3, pp. 727–728.

[14] C. P. Tsekrekos, R. W. Smink, B. P. de Hon, A. G. Tijhuis, and A. M. Koonen, "Near-field intensity pattern at the output of silica-based graded-index multimode fibers under selective excitation with a single-mode fiber," vol. 15, no. 7, pp. 3656–3664, 2007.

[15] M. Awad, I. Dayoub, A. Okassa-M'foubat, and J.-M. Rouvaen, "The inter-modes mixing effects in mode group diversity multiplexing," *J. Opt. Commun.*, vol. 282, no. 19, pp. 3908–3917, 2009.

[16] M. Awad, I. Dayoub, A. Okassa, J.-M. Rouvaen, and J.-P. Vilcot, "Radio on optical fiber and multi-sevices in single-MMF LAN using mode group diversity multiplexing," in *3rd Int. Conf. on Information and Communication Technologies*, 2008.

[17] R. W. Heath Jr., S. Sandhu, and A. J. Paulraj, "Antenna selection for spatial multiplexing systems with linear receivers," *IEEE Commun. Lett.*, vol. 5, no. 4, pp. 142–144, 2001.

[18] C. P. Tsekrekos, M. de Boer, A. Martinez, F. M. J. Willems, and A. M. J. Koonen, "Temporal stability of a transparent mode group diversity multiplexing link," *IEEE Photon. Technol. Lett.*, vol. 18, no. 23, pp. 2484–2486, 2006.

Mazen Awad was born in Hermel, Lebanon, in 1981. He received the M.Sc. and Ph.D. degrees in electronics and telecommunications from the University of Valenciennes, France, in 2005 and 2010, respectively. Currently he is a Postdoctoral Researcher at the IEMN/DOAE at the University of Valenciennes, France. His research interests are focused on optical network design, RoF systems, and optical MIMO technology.

Iyad Dayoub received the M.A.Sc. in electrical engineering from the University of Nancy (Polytechnic Institute), Nancy, France, in 1997, and the Ph.D. degree in telecommunications from the University of Valenciennes, France, in 2001. In Sept. 2003, he joined the Department of Opto Acoustic and Electronics at the Institute of Electronics, Microelectronics and Nanotechnology (IEMN/DOAE), University of Valenciennes, France, where he is currently an Associate Professor. His research activities are developed with the Digital Communications Group of the IEMN, including wireless communications, emerging wireless access technologies, hybrid radio optic networks, optical MIMO, and signal detection and estimation. Since 2007, he has been a member of the National Council of Universities, France, in the area of electrical engineering, electronics, photonics, and systems.

Walaa Hamouda received the M.A.Sc. and Ph.D. degrees in electrical and computer engineering from Queen's University, Kingston, ON, Canada, in 1998 and 2002, respectively. In July 2002, he joined the Department of Electrical and Computer Engineering, Concordia University, Montreal, QC, Canada, where he is currently an Associate Professor. Since June 2006, he has been the Concordia University Research Chair in Communications and Networking. His current research interests include wireless networks, MIMO space–time processing, optical MIMO, and source and channel coding. Dr. Hamouda has received many awards, including the best paper award (WNS) of the 2009 International Conference on Communications (ICC09) and the IEEE Canada Certificate of Appreciation in 2007 and 2008. He served as the Technical Co-chair of the Ad hoc, Sensor, and Mesh Networking Symposium of the 2010 IEEE ICC and the 25th Queen's Biennial Symposium on Communications, as well as the Track Chair for the Radio Access Techniques of the Fall 2006 IEEE Vehicular Technology Conference. From September 2005 to November 2008, he was the Chair of the IEEE Montreal Chapter of Communications and Information

Theory. He serves as Associate Editor for the *IEEE Transactions on Vehicular Technology*; *IEEE Communications Letters*; *IET Wireless Sensor Systems*; *Wiley International Journal of Communication Systems*; and *Journal of Computer Systems, Networks, and Communications*.

Jean-Michel Rouvaen was born in Maubeuge, France, in 1947. He received his Ph.D. degree in electronics from the Universities of Paris VI and Valenciennes, France, in 1976. Currently he is a Professor at the University of Valenciennes, France, where he teaches electronics, signal processing, and telecommunications. Previously, he was involved in ultrasonics and acousto-optics. His current research interests are focused on telecommunication systems and their application to security in intelligent transportation systems.